Electrochimica Acta 563 (2026) 148733

Contents lists available at ScienceDirect

Electrochimica Acta

journal homepage: www.journals.elsevier.com/electrochimica-acta

Thermodynamic stability of single-atom catalysts in electrochemical conditions from first principles: Role of the local coordination

Matteo Spotti [1], Clara Saetta [1], Mesfin Eshete [1], Giovanni Di Liberto [*]

Department of Materials Science, University of Milano-Bicocca, Via Cozzi 55, 20125 Milano, Italy

ARTICLE INFO

Keywords:
DFT
SAC
HER
Pourbaix diagram

ABSTRACT

Single-Atom Catalysts (SACs) are a hot topic in catalysis research. Nowadays, there is a growing attention in modelling the reactivity and activity of SACs towards several electrochemical reactions. The activity of SACs is strongly sensitive to the local coordination of the transition metal atoms. An aspect less explored is assessing their stability in electrochemical conditions. In this work, we performed a density functional theory investigation of SACs based on MoS_2, a widely adopted supporting material, by focusing on the role of the local coordination to the stability. Our results are based on a dataset of fifteen transition metal atoms on four different possible coordinative sites. The stability of SACs in electrochemical conditions is predicted by using a recently proposed simple yet practical scheme within the formalism of Pourbaix diagrams [*ACS Catal. 14, 45 (2024)*]. When looking at the role of the metal, Pt-SACs are mostly stable, compatible with the large diffusion of these kinds of systems in experiments. Results show that the local coordination has a dramatic effect on stability. Most often the simple adsorption of metals on MoS_2 leads to unstable systems, unless noble atoms are considered. Moreover, stability improves when metal atoms occupy lattice S sites, but the most stable configurations refer to substitutional doping of Mo atoms. The results provided are validated against selected available experimental data. These results provide a further example of the crucial role of the local coordination in single-atom catalysis and may of help for the screening of potential candidates and could be used to help the understanding of the active phase in promising electrocatalysts.

1. Introduction

Single-atom catalysis is a relatively new frontier in catalysis research, with a broad spectrum of potential applications, ranging from the activation of stable molecular systems such as carbon dioxide, water and nitrogen to organic synthesis for pharmaceutics [1–4]. A single-atom catalyst (SAC) is a material made by transition metal atoms (TMs) atomically dispersed on the surface of a supporting matrix [5,6]. These objects are particularly interesting as they bridge to a certain extent the classical worlds of homogeneous and heterogenous catalysis [7,8].

Two-dimensional materials have emerged as promising supporting agents due to their layered structure and potential applicability in electrochemical conditions [9,10]. Among these materials, molybdenum disulfide (MoS_2) has gathered significant attention due to its potential applications in various fields [11–13].

A series of seminal studies demonstrated the potential of SACs supported on MoS_2 [14–17]. Nowadays, there is vast plethora of successful examples of the use of MoS_2-based SACs. To name a series of seminal studies, Lang et al. used Ru single atoms supported on defective MoS_2 for HER, reaching a lower overpotential for hydrogen evolution with respect to commercial MoS_2: 107 mV vs 364 mV at 10 $mAcm^{-2}$ [18]. Deng et al. successfully synthetized Pt-doped MoS_2 and used in HER by embedding the metal atom in a molybdenum vacancy [19]. Similarly, Ma et al. designed Ni- and Co-based single atoms in molybdenum site with adjacent sulfur vacancy [20]. These electrocatalysts showed excellent activity for HER and OER in alkaline conditions, with overpotentials of about 101 and 190 mV at 10 mA cm^{-2}, respectively. Other works such as the one of Zou et al. showed also activity for CO_2 reduction on substitutional sites of MoS_2 [21].

Quantum chemical simulations are often used not only to provide an atomistic description of the chemistry behind SACs, but to scrutinize databases, a step of the so-called rational design of promising candidates. For instance, several studies have examined the ability of SACs

* Corresponding author at: Università Milano-Bicocca, Dipartimento di Scienza dei Materiali, via R. Cozzi 55, 20126 Milano.
E-mail address: giovanni.diliberto@unimib.it (G. Di Liberto).
[1] MS, CS and ME contributed equally.

https://doi.org/10.1016/j.electacta.2026.148733
Received 29 January 2026; Received in revised form 18 March 2026; Accepted 24 March 2026
Available online 25 March 2026

supported by MoS_2 to activate inert molecules such as CO_2 and N_2 [22–26].

In this context it is essential to underline the main contribution of this work and the main take-home messages. Typically, the attention of screening is posed on assessing the reactivity and activity of SACs towards desired reactions. Recently, it is emerging another aspect of key importance, the stability of SACs in electrochemical conditions. This aspect is widely known in computational electrochemistry and our work contributes in underlining the importance of predicting stability in the field of single-atom catalysis. Stability assessment is somewhat preliminary with respect to reactivity, for a broad spectrum of chemical processes ranging from the activation of small molecules to the development of composite catalytic systems for industrial-scale sustainable chemistry, an aspect highlighted by Tian et al. [27]. It must be underlined that the stability of SACs can strongly differ from the bulk metal counterpart, as metal atoms are coordinated to ligands. The widespread reliance on binding energy in DFT studies of SACs reflects a trade-off between computational tractability and accuracy. While binding energy provides a useful first-order descriptor for metal-support interaction, it fails to account for environmental effects and support heterogeneity, which ultimately determine catalyst stability under realistic conditions. For this reason, Pourbaix Diagrams can play as a helpful tool in the field of electrocatalysis. Recently, some of us proposed a very simple yet-practical scheme to predict the stability of SACs in electrochemical conditions, based on thermodynamics consideration in the framework of Pourbaix diagrams [28]. Later, Exner, Viñes, Illas and co-workers proposed a similar strategy focused on the stability of catalysts in anodic polarization conditions [29,30]. MoS_2 is a particularly interesting case, as transition metal atoms can be incorporated in the matrix, basically in four different ways, ranging from simple adsorption on the surface to substitution of the metal or non-metal atom [31,32]. The stability of a given metal atom in such very different environments is expected to be dramatically affected.

In this work, we assess the stability of MoS_2-based SACs by investigating a database of 15 transition metal atoms (V, Cr, Mn, Fe, Co, Ni, Cu, Ru, Rh, Pd, Ag, Os, Ir, Pt and Au) embedded in MoS_2 and focusing on four common adsorption configurations: *i)* adsorption of the metal atom on the surface, here denoted as TM@MoS_2 [15,22,33–35]; *ii)* substitutional doping by adsorption on sulfur vacancies, here denoted as TM_S@MoS_2 [17,36,37]; *iii)* adsorption on a Mo vacancy, here denoted as TM_{Mo}@MoS_2 [38,39]; *iv)* Mo substitutional doping in the presence of a sulfur vacancy, here denoted as TM_{MoS}@MoS_2 [14,20]. Here, we are interested in evaluating the stability of the system under operating conditions. In other words, we are not looking synthesis stability, which is relevant under high-temperature conditions, but rather electrochemical stability. This is often referred to as the stability of the system operating at (most often) room temperature under potential- and pH-dependent conditions. We simulated the stability of SACs as a function of applied voltage and pH against dissolution, by considering the formation of common species in reducing and oxidation reactions in aqueous environment, such as H*, OH*, O* and OOH*.

Results indicate that the local coordination determines the stability of the SACs. Importantly, SACs involving simple adsorption or replacing S vacancies are much less stable than those replacing a Mo atom on the surface. As a result, the latter systems are most often predicted as stable in electrochemical conditions. Of course, despite the message is general, it also depends on the nature of the metal. The results are finally validated against available experimental results and can be used to contribute in providing a description of the nature of the active phase in experimental samples for which the assignment of the active phase is unclear. This study further underlines the importance of assessing the stability of SACs besides the reactivity. The study also contributes into highlighting how essential it is knowing the local coordination of SACs with atomistic detail.

2. Computational methods

We performed density functional theory (DFT) calculations as implemented in VASP simulation package [40–42]. The Perdew-Burke-Ernzherov (PBE) exchange-correlation functional was used [43]. All calculations include spin polarization. Dispersion interactions were accounted by means of Grimme's D3 scheme [44]. Valence electrons were expanded on a set of plane waves with a working kinetic cutoff equal to 400 eV, whereas core electrons were treated by Plane Augmented Wave (PAW) pseudopotentials [45,46]. We benchmarked the cutoff value by performing test calculations with an increased cutoff of 500 eV, Section S3.2. Even though MoS_2 is a semiconductor, previous studies show that PBE functional is commonly adopted to compute structural properties, therefore we did not apply the Hubbard correction on Mo atoms (see Section S3.1) [47,48]. PBE0 single point calculations were performed to account for the self-interaction error and refine the electronic structure [49]. This strategy avoids energy intensive optimizations with hybrid functionals and allows at the same time to improve the description of the electronic structure with reasonable accuracy [50,51]. It must be underlined that one must we aware that this is an approximation. However, in the field of SACs, we extensively and deeply tested the approximation over the last few years, finding that it represents a suitable and reliable trade-off between accuracy and computational effort, with errors of about 0.1 eV [51]. Another alternative strategy is the adoption of the DFT+U approach, where an ad-hoc correction is used on d orbital of transition metal atoms. We performed a few benchmark simulations, Section S3.1, finding that the use of $+U$ allows to partially reconcile PBE estimates with PBE0, an aspect that we already reported in previous works [50,52]. We are aware that novel functionals are now arising in the DFT panorama, one of them, R2SCAN [53], demonstrated very promising. We, therefore, performed benchmark calculations of selected cases, as reported in Section S3.4.

The binding energy of the metal atoms (E_b) was calculated by taking as a reference the support (E_S) and the free metal atom, $E_{M,}$ Eq. (1). This property is used as a proxy to assess the stability of SACs [54–56].

$$E_b = E_{M@S} - (E_M + E_S) \quad (1)$$

The Gibbs free energy of chemical intermediates (H*, OH*, O*, OOH*) was evaluated by using the Computational Hydrogen Electrode (CHE) approach [57,58], calculating the binding energy from DFT reaction energies (ΔE), and considering thermodynamic corrections as entropic ($T\Delta S$) and zero-point energy contributions (ΔE_{ZPE}), as reported in Eq. (2). The effect of pH and voltage was approximated as reported below. The Gibbs free energy of a species x is calculated as:

$$\Delta G_x = \Delta E_x - T\Delta S_x + \Delta E_{ZPE} - n_{H^+} 0.0592pH - n_e E \quad (2)$$

n_{H^+} and n_e are the number of protons and electrons exchanged, respectively, and E is the applied voltage with respect to the Standard Hydrogen Electrode (SHE). The working quantities are reported in Table S1. We considered in this work the formation of H*, OH*, O* and OOH*. All calculated Gibbs free energies are reported in Table S2.

The vibrational entropy of solid-state species was computed through the formalism of the partition function within the harmonic approximation [59]. The zero-point energy contribution was estimated in a harmonic fashion, allowing to vibrate the atoms of the chemical intermediate of interest and the metal atom [60,61]. The treatment of solvation goes beyond the specific purpose of the study. Nevertheless, solvent effects can be added to the calculation of stability diagrams. If the solvent is treated with implicit solvation schemes usually the effect is small [28], although it is certainly system dependent. We tested selected systems with implicit solvation by using the VASPsol implementation [62,63] and dielectric constant of water. The results show energy changes with respect to within 0.2 eV, see Section S3.3. Based on this result we performed the rest of the study neglecting implicit solvation. It must be emphasized that the treatment of water would imply the use of

complicated and often demanding approaches, to account for its dynamical and fluxional nature [52,64–67].

We started from the fully optimized unit cell of bulk crystal structure of 2H-MoS_2 ($a = b = 3.19$ Å, $c = 13.38$ Å and $\gamma = 120°$). We focus on the 2H-phase of MoS_2, which is the one used in a series of studies on SACs [16,18,19,68]. We modelled a monolayer and optimized a $3 \times 3 \times 1$ supercell. A vacuum layer of about 3 nm thick was added to avoid spurious effects due to interaction between periodic replica along the non-periodic direction. The optimized lattice parameters are: $a = b =$ 9.498 Å, and $\gamma = 120°$ The use of such a supercell allows to model SACs with a reasonable concentration of metal atoms, compatible with real samples. The SAC models were created as follows. In one case, metal atoms were adsorbed on the surface, Fig. 1a. In a second case, we generated a sulfur vacancy and replaced it with the dopant metal atom, Fig. 1b In the third case, the transition metal atom was put in place of Mo, Fig. 1c. Finally, the metal atom replaced Mo in the proximity of a sulfur vacancy, Fig. 1d

As mentioned above, we do not explicitly consider the direct effects of applied potential and pH in this work. This could be done by invoking Grand Canonical approaches, where the role of extra electrons and protons is taken under consideration [69–71]. This aspect would go beyond the specific purpose of the study, and for this reason we restrict our computational scheme to the commonly adopted indirect effect of both pH and applied voltage, Eq. (1).

3. Results and discussion

3.1. Calculating Pourbaix diagrams of SACs

We start by recalling the main steps to determine the stability diagrams of SACs in electrochemical reactions. As mentioned above, a suitable approach is based on Pourbaix diagrams [72,73] where the most stable species is identified for a given value of pH and applied potential (E). In the general formulation of Pourbaix diagrams of bulk materials, one must consider a series of possible dissolution processes and calculate the Gibbs free energy of the different species under consideration. In the case of SACs, it is necessary also to account for the interaction between the metal and supporting matrix. Recently, we suggested a simple, yet practical scheme reported in Fig. 2 [28]. We see that the Gibbs free energy for a given dissolution process can be described by summing three different contributions.

$$\Delta G_{diss} = -E_b - E_c + \Delta G_{redox} \quad (3)$$

At first, one must spend energy to separate the metal by the supporting materials; this corresponds to the opposite of the binding energy of the metal, - E_b. Here we defined the binding energy as the difference between the total energy of the single-atom catalyst system and the energies of the defective support and the reference isolated metal atom (Eq. (1)). Then, the second term is the opposite of cohesive energy, - E_c. Cohesive energy is the energy gain to move from metal bulk to an isolated metal atom. The remaining term is the classical oxidation Nernstian process describing the dissolution of a metal, ΔG_{redox}. The reference state for Gibbs free energy of the oxidation process is the bulk metal, with final state metal ions in water, hydroxides, oxides, or anion with the metal in a high-oxidation number. It is computed as $\Delta G_{redox} = n_e F E_{redox}$. We assume that all species are at standard concentration. It is known that the binding energy can be used as a proxy for stability for SACs. Indeed, in this framework, two quantities can be taken from experimental values [74], and the binding energy only must be evaluated from first principles [28]. The experimental cohesive energies and redox processes of all metals are reported in section S2. The more negative the energy is, the more stable the SAC will be, as dissolution processes will have higher Gibbs free energy. At the same time, it is also possible to observe that the dissolution free energy of a single atom in a

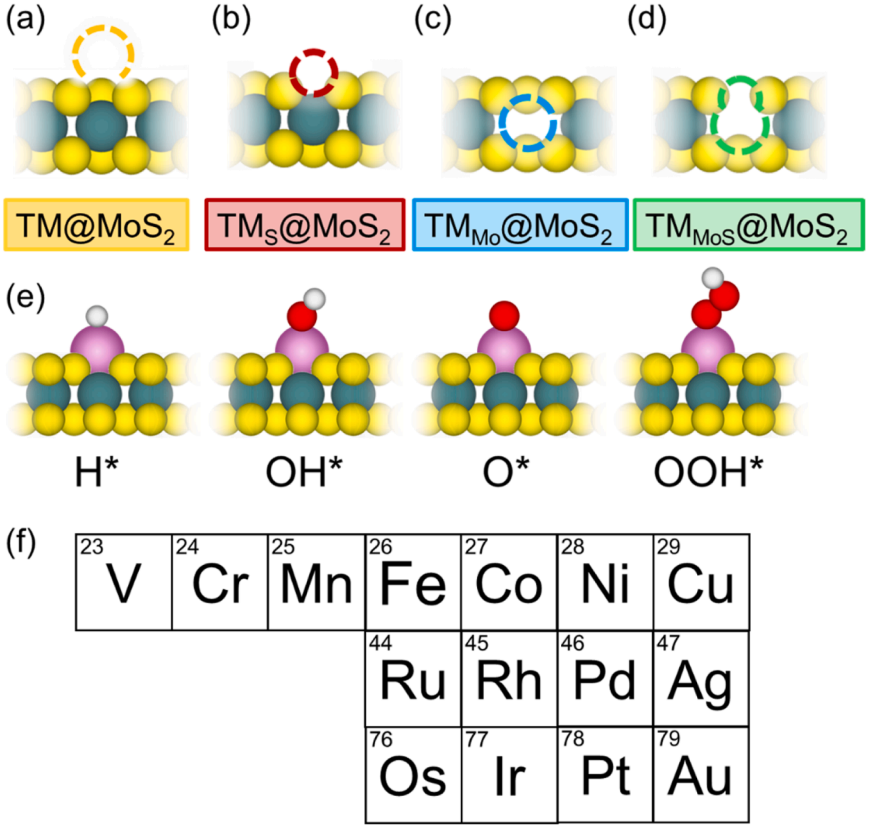

Fig. 1. Panels(a)-(d) show the four different configurations assumed by metal atoms studied in this work. Panel (e) sketches the chemical species considered H*, OH*, O*, OOH* that could form in electrochemical conditions of applied pH and voltage. Panel (f) reports the TM atoms considered in this work.

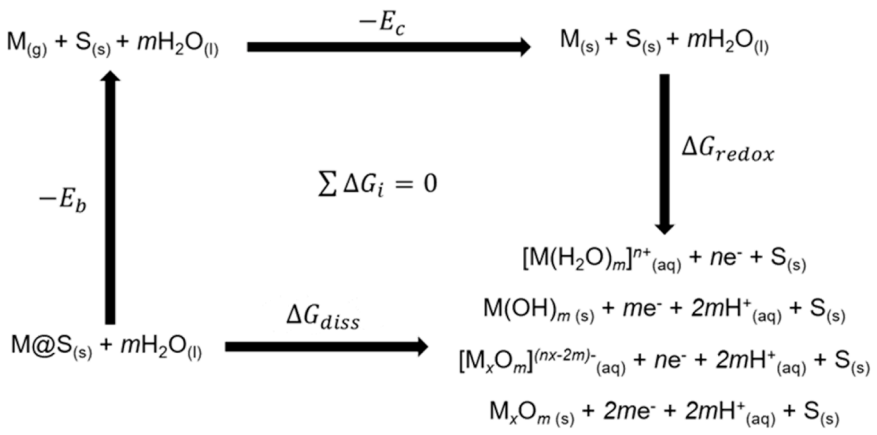

Fig. 2. Thermodynamic cycle to determine dissolution Gibbs free energy. The SAC can undergo dissolution and form metal ions in water, hydroxide, oxides, or anion with the metal in a high-oxidation number.

matrix, ΔG_{diss}, and the corresponding counterpart of the bulk metal, ΔG_{redox}, differ, as both binding energy and cohesive energy are involved. This explains the observed stability of transition metal atoms atomically dispersed in matrices [75], such as Fe, that would be unstable electrochemically otherwise. This strategy allows to reduce the complexity of the framework to a single calculated quantity, which can be considered the descriptor for the stability; the binding energy of the metal atom to the support. It must be considered, that this is an approximation, especially since cohesive energies and redox potentials are equally important, and they are taken from experimental values, as done for equilibrium potentials of reactions in CHE. This introduces unavoidable approximations. For instance, in the case of cohesive energies, Illas and co-workers reported that the calculation of bulk cohesive energies is a quest with density functional theory [74]. For this reason, we preferred to adopt, when available, experimental values.

Before discussing stability diagrams of SACs, we first analyze the binding energies of metal atoms in different coordination, Fig. 3. In the case the metal atom is embedded in a vacancy, we assume that the support has available vacancies, which is a reasonable assumption. In general, binding energies depend on both the nature the metal atom and its local coordination. The calculated values are reported in Table 1. In the case of MoS_2-based SACs, the coordination is extremely important. When the metal atom is adsorbed to the surface of MoS_2, it corresponds to least stable configuration. Except for Pt, which shows $E_b = -4.1$ eV, E_b is always as low as −3 eV. Such high values can be explained in the light of the relative undercoordinated nature of the metal atom, which is characterized by three contacts with S atoms, Figure S1a. If the metal atom is instead replacing a sulfur vacancy, the binding energies are in general more negative, ranging from −3.5 eV (Ag) to −7.6 eV (Pt). In

Table 1
Binding energies of transition metal atoms in different sites.

	E_b /eV			
	$TM@MoS_2$	$TM_S@MoS_2$	$TM_{Mo}@MoS_2$	$TM_{MoS}@MoS_2$
V	−1.95	−4.92	−13.23	−12.79
Cr	−1.31	−3.91	−10.55	−9.96
Mn	−0.60	−3.84	−8.57	−7.96
Fe	−1.35	−3.86	−8.35	−7.83
Co	−1.65	−3.97	−7.87	−7.70
Ni	−2.78	−4.64	−8.16	−7.90
Cu	−1.81	−3.93	−6.32	−5.97
Ru	−3.64	−6.53	−13.00	−13.01
Rh	−3.70	−6.45	−11.31	−10.87
Pd	−2.67	−5.11	−7.53	−7.30
Ag	−1.44	−3.49	−4.74	−4.67
Os	−2.18	−5.47	−13.63	−13.61
Ir	−2.62	−6.02	−11.71	−11.78
Pt	−4.07	−7.59	−10.92	−10.63
Au	−1.94	−4.30	−5.70	−5.34

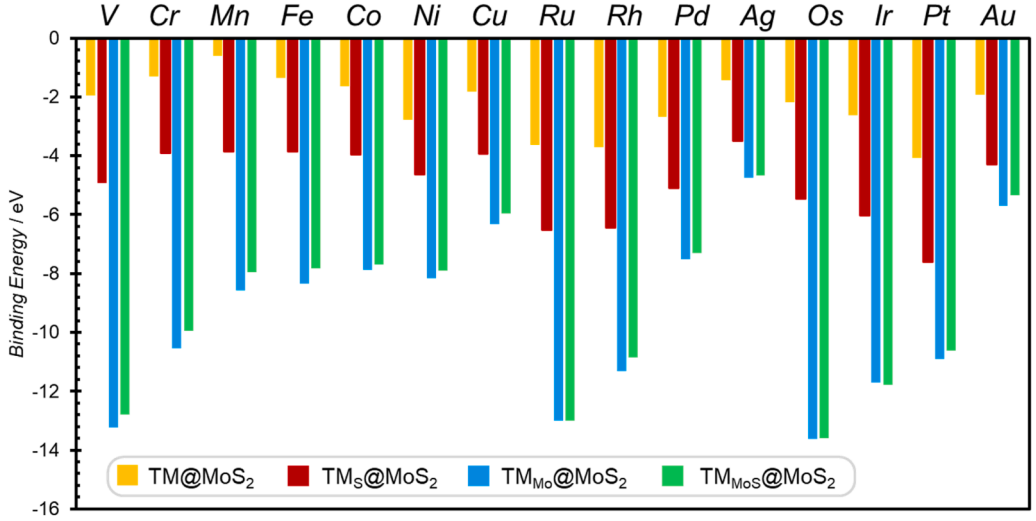

Fig. 3. Calculated binding energies of transition metal atoms on different possible sites of MoS_2; adsorbed metal atoms (yellow), metal atoms replacing a S atom (red), metal atom replacing a Mo atom (light blue), the same but having a S vacancy in the proximity too (green).

this case, the metal atom displays three contacts with Mo atoms, Figure S1b. The situation improves further when considering the metal atoms in place of Mo sites. This is expected as the most favorable condition as the dopant atom replaces a metal atom of the matrix and assumes its coordination site. Indeed, the calculated binding energies span from −4.8 (Ag) to −13.2 eV (V). Finally, the coordination of the metal atom is only weakly affected by the presence of an S vacancy in its proximity, resulting in small changes of the binding energies.

In this work, we focus on a strategy to extract stability diagrams and on the implications of stability. Therefore, we do not focus on the origin of different binding energies with electronic structure descriptors. Nevertheless, electronic structure descriptors can provide additional information to the origin of different binding energies. Examples are atomic charges and d-band center. In the first case, it has been reported that electron counting is problematic in solids, but it allows to extract qualitative information [76]. At the same time, in SACs the concept of d-band center needs to be reconsidered close to d-orbital one, due to the single-site character of the metal atom. Therefore, the rationalization of electronic structure descriptors is not trivial in single-atom catalysis [51, 77].

As representative example we discuss the Pourbaix diagrams of Fe and Ni in two different situations, when the metals are adsorbed on the surface, Figs. 4a-b, and when they are substituted in place of Mo, Figs. 4c-d. If we start from Fe@MoS_2 (Fig. 4a), we see that the metal atom is expected to dissolve in any condition investigated in this study, $0 < pH < 14$ and $-1\ V\ (vs\ SHE) < E < 2\ V\ (vs\ SHE)$. Moving to Ni@$MoS_2$, we observed that in acidic and reducing conditions the SAC is stable, identified by a * in Fig. 4b, but it tends to dissolve when either increasing the potential in oxidation or increasing the pH. The higher stability of Ni@MoS_2 with respect to Fe@MoS_2 can be understood by values of E_b, E_c, and the redox potentials of couples involving the two metals [28].

The picture changes completely when considering Fe_{Mo}@MoS_2 and Ni_{Mo}@MoS_2. Indeed, the iron atom is expected to be significantly more stable, undergoing dissolution only at moderate to high values of applied potential and pH, Fig. 4c. As a reference, we report with dashed lines the equilibrium values of the redox curves of H_2 and O_2 water splitting semi-reactions. We see that the Fe atom is expected to be covered by H* in reducing conditions, and it will gradually become uncovered and then bound to OH* when increasing the potential. At high oxidation potential the metal will dissolve leading to Fe^{3+} or highly oxidized states. A similar discussion applies to Ni_{Mo}@MoS_2, where the stability window is even larger, Fig. 4d In this case, the SAC is predicted

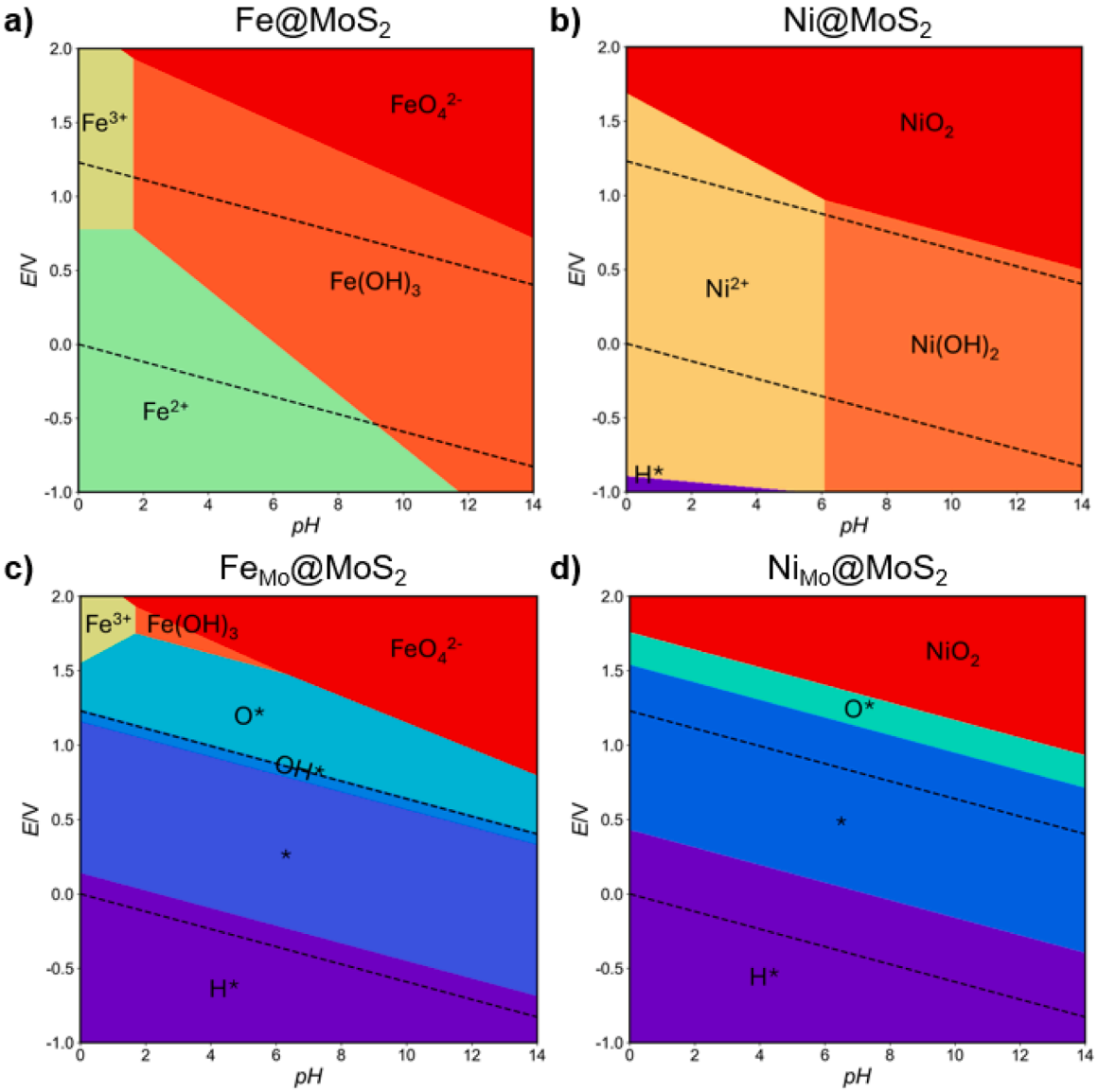

Fig. 4. Simulated Pourbaix diagrams of (a) Fe@MoS_2, (b) Ni@MoS_2, (c) Fe_{Mo}@MoS_2 and (d) Ni_{MoS}@MoS_2.

stable is all the thermodynamic window of water splitting reaction. If we compare the same metal atom in different coordination, such as Fe@MoS_2 vs Fe_{Mo}@MoS_2 or Ni@MoS_2 vs Ni_{Mo}@MoS_2 the different stability arises from changes in its binding energy. In the case of Fe, E_b moves from −1.35 eV to −8.35 eV for Fe@MoS_2 and Fe_{Mo}@MoS_2 respectively, a dramatic change. Similarly, E_b is −2.78 eV in Ni@MoS_2, that becomes −8.16 eV when taking Ni_{Mo}@MoS_2.

Another instructive example is that of cobalt, Fig. 5. When the metal is adsorbed to the surface of MoS_2, Fig. 5a, it is expected that it will dissolve, similar to Fe@MoS_2. The situation improves when having Mo_S@MoS_2 (Fig. 5b), as we have seen before that the binding energy becomes more negative. In this case, the SAC is stable in reducing conditions, but it will tend to dissolve when increasing the pH and when going to $E > 0$ V (vs SHE). Again, the picture changes when considering the metal in place of Mo, Fig. 5c. In this case, the SAC is stable against dissolution; it is expected to dissolve only at very high pH values and strong oxidizing conditions. The presence of a sulfur vacancy in proximity of the cobalt atom has a small effect (0.17 eV) on the binding energy (Table 1), as discussed before. This is reflected in small changes in the stability diagram, Fig. 5d

All calculated Pourbaix diagrams are reported in Figures S2-S61. We summarize the overall trends as reported in Fig. 6. We defined a grid of pH values for two representative and arbitrary potential regimes, where we extracted if the SAC would tend to dissolve or not. To evaluate the stability of the system in HER conditions we selected $E = 0$ V vs RHE, and for HER/OER conditions $0 \leq E \leq 1.23$ V vs RHE. It is evident that when the majority of metals (among those investigated in this work) are adsorbed on MoS_2, they will dissolve in any condition. Only a few exceptions survive, represented by noble metals. Moving to other coordinations where the metal is replacing S atom, there is an improvement, although it is dependent on the specific nature of the metal. Then, if the single atom is replacing Mo, there is a more general and systematic picture, where the SACs will be stable against dissolution. This result is consistent with previous works showing that typically, the binding energy of a TM resulting in stable SACs must be more negative than 4 eV, i.e. $E_b < -4$ eV [28,60]. These results indicate that in real samples, it could be unlikely that transition metal atoms will simply adsorb on MoS_2, while they will tend to occupy coordination sites, left by S vacancies, or most probably by replacing Mo atom. It should be noted that the stability map presented in Fig. 6 is based on a thermodynamic criterion and therefore provides a binary classification of stable versus unstable configurations according to the chosen stability

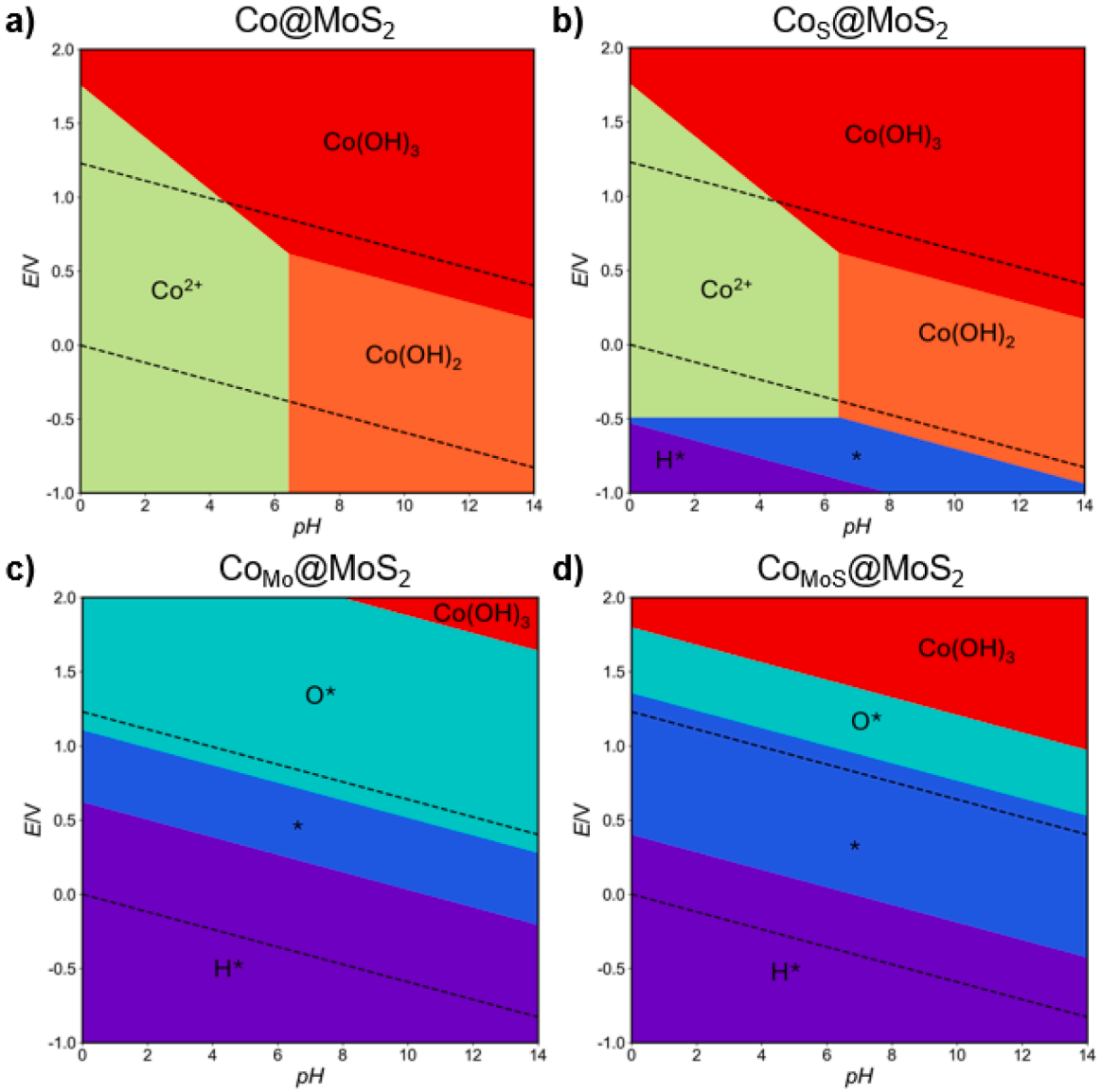

Fig. 5. Simulated Pourbaix diagrams of (a) Co@MoS_2, (b) Co_S@MoS_2, (c) Co_{Mo}@MoS_2 and (d) Co_{MoS}@MoS_2.

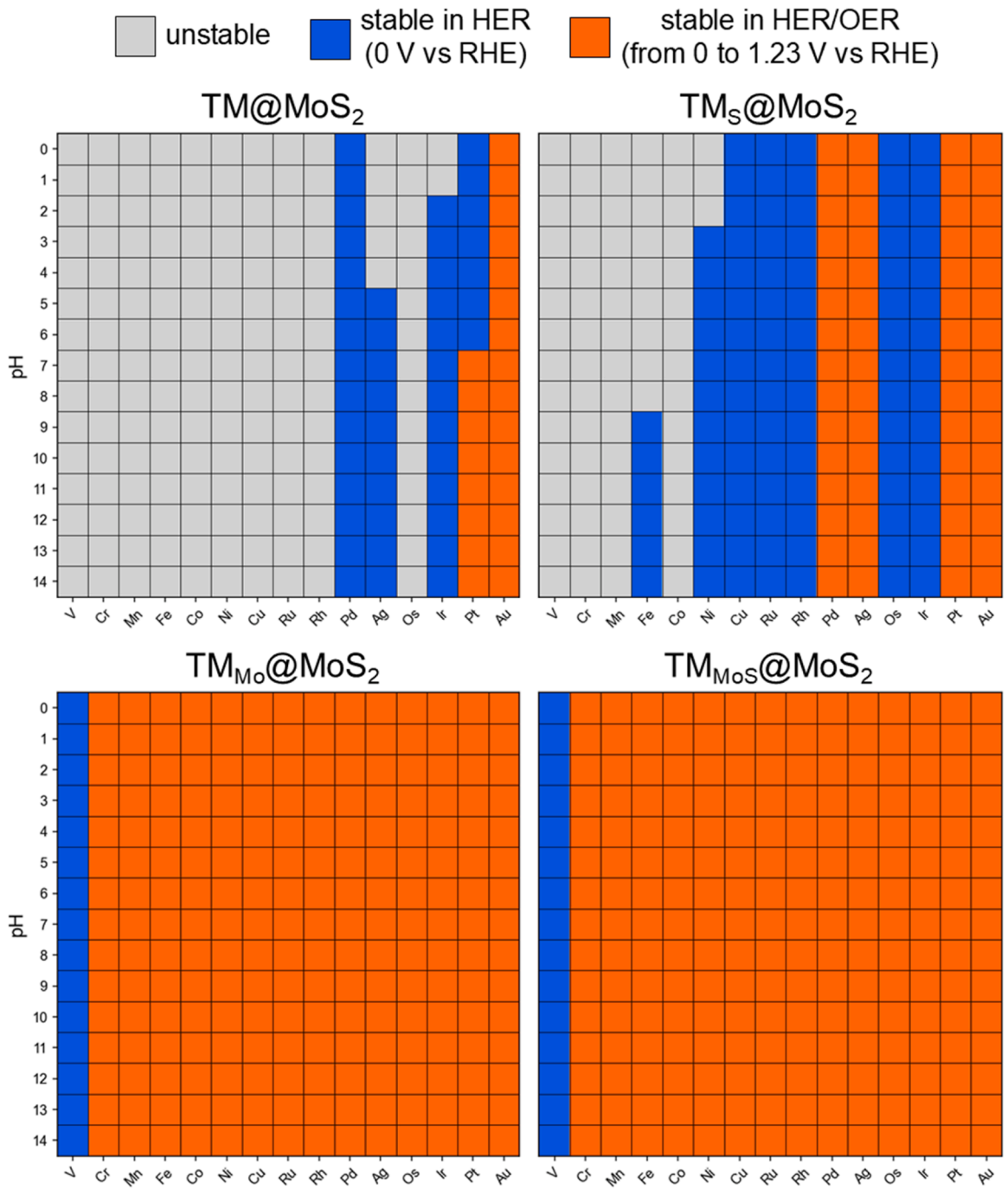

Fig. 6. Predicted stability of all simulated single-atom systems at different pH values. Grey stands for dissolved catalytic systems, in blue stable systems in HER conditions, where we selected the value of applied potential equal to 0 V vs SHE. In red we report stable systems from 0 V to 1.23 V vs SHE, referred as stable in HER/OER conditions.

threshold. Systems located close to this boundary should be interpreted with caution, as their persistence under electrochemical conditions may depend on kinetic barriers to dissolution or restructuring that are not captured within the present thermodynamic framework.

In this work we focused our attention on the basal plane structure of MoS_2. However, in the literature are reported examples of MoS_2 edge planes that show activity without the need of a dopant metal [78,79]. We decided to perform a few additional calculations to extend our results to selected edge sites. We focused on Pt-based SACs. The details of the calculations are reported in Section S4. Interestingly, Pt embedded in edge sites lead to very stable adsorbate, which provide very stable SACs in a broad pH-*E* window. Motivated by this result, we aim at performing a future study devoted to investigation of SACs supported on edge sites to provide also some insight into the role of different local coordination between basal and edge sites of MoS_2.

3.2. *Implications in experiments*

In this last section we assess the reliability of our predictions against experimental data. It must be said that this part is not straightforward, as quantum chemical data can be predicted only if the model is sufficiently close to what is present experimentally [80,81]. We have seen that Pt-SACs are particularly stable, especially when the metal atom occupies Mo substitutional sites, Figure S45. This is in line with a recent work

[19]. by Deng et al. The authors successfully prepared Pt atoms atomically dispersed on MoS_2, where Pt atoms preferentially substitute Mo atoms. The system was applied in HER at pH = 1 operating from 0.2 to −0.7 V vs RHE. In addition, Han et al. [82]. prepared MoS_2-based SACs by depositing Co, Ru, and Ni atoms in Mo vacancies and used them for HER at pH=10. Based on our results, only substitutional models for Co, Ru and Ni are compatible with experiments, as one could expect the metal to dissolve otherwise, Figures S36–37 and S39. It must be said that these considerations neglect kinetic effects, as they rely on thermodynamic considerations only. Another example is Ru@MoS_2. In a recent study, Lang et al. [18]. prepared Ru@MoS_2 and used it for HER in a pH = 14 solution from 0 to −0.5 V vs RHE. The authors observed the simultaneous presence of Ru atoms substituting Mo ones, and a small amount of Ru atoms occupying S sites. Our calculated diagrams agree with this interpretation, as the most likely configurations consist of substitutional Mo, and Ru_S@MoS_2 is possible in HER conditions, Figures S24 and S39. On the other hand, adsorption of Ru is not possible both experimentally and theoretically, Figure S9. Furthermore, the synthesis of Ni and Co single atoms embedded in a Mo site near a S vacancy has also been experimentally verified by Ma et al. [20], with which HER and OER were performed in a pH = 14 solution from 0 to −0.4 V vs RHE ad from 1.2 to 1.8 V vs RHE, respectively. Our simulated diagrams demonstrate the stability of these systems under alkaline HER and OER conditions, Figures S51–52 .

Besides testing the reliability of the calculations, the results could be used, in principle, to assist the understanding of the nature of the local coordination of the SACs. Furthermore, our results indicate that simple adsorption of transition metal atoms is in general unlikely. These findings may have implications in computational screening studies of big databases. Finally, further work will be devoted in extending the study to other possible configurations, involving for instance edge defects.

4. Conclusions

We performed quantum chemical density functional theory (DFT) calculations to predict the stability of single-atom catalysts (SACs) supported on MoS_2 in electrochemical conditions. We investigated a dataset of 15 (V, Cr, Mn, Fe, Co, Ni, Cu, Ru, Rh, Pd, Ag, Os, Ir, Pt and Au) transition metal atoms, and considered four possible and widely investigated coordination sites. We considered *i)* the adsorption of metal atoms on the surface of materials, *ii)* the occupation of lattice sites left by S-vacancies, *iii)* the occupation of Mo sites, and *iv)* the same but in the proximity of a S vacancy. The stability was assessed by evaluating Pourbaix diagrams of SACs by using a recently proposed simple strategy, which accounts for the binding energy of the metal atoms, i.e. how strong is the interaction with the matrix. In the case of MoS_2, the very different coordination of the metal atom reflects dramatic changes in adhesion energies, which influences the stability in electrochemical condition. The results provided are validated against available experimental data. Except for some noble metals, the simple adsorption is predicted as unlikely, due to the insufficient interaction of the metal atoms with the matrix. This suggests that in real samples simple adsorption may be complex to achieve, an important aspect when aiming at performing screenings to find promising candidates. The stability can be improved by incorporating the metal in S vacancies, while the results are still dependent on the nature of the metal atom. The situation changes when investigating metal atoms occupying Mo sites. In this case, there is always a strong interaction between the metal atoms and the matrix, which results in always electrochemically stable objects in both reducing and oxidation conditions. The simultaneous presence of S vacancies in the proximity of metal atoms has a small but not negligible effect. The results of this study not only provide further insight into the understanding of MoS_2-based SACs, but they can be used as an example of the key importance of considering the local coordination of the metal atoms. Understanding how the coordinative environment influences the electronic properties of the metal site, such as the oxidation state, is crucial for the description of the performance of a catalyst under operating conditions [83]. The prediction of stability of SACs demonstrates a prerequisite to investigating prior assessing the activity and reactivity of SACs. Future work will be devoted to the full and detailed assessment in the field of single-atom catalysis of novel DFT functionals that demonstrated promising results.

Author information

Matteo Spotti (MS), Dipartimento di Scienza dei Materiali, Università di Milano-Bicocca.

Clara Saetta (CS), Dipartimento di Scienza dei Materiali, Università di Milano-Bicocca.

Mesfin Eshete (ME), Dipartimento di Scienza dei Materiali, Università di Milano-Bicocca.

CRediT authorship contribution statement

Matteo Spotti: Writing – review & editing, Investigation, Data curation, Conceptualization. **Clara Saetta:** Writing – review & editing, Investigation, Data curation, Conceptualization. **Mesfin Eshete:** Writing – review & editing, Investigation, Data curation. **Giovanni Di Liberto:** Writing – review & editing, Writing – original draft, Supervision, Project administration, Funding acquisition.

Declaration of competing interest

The authors declare that they have no known competing financial interests or personal relationships that could have appeared to influence the work reported in this article.

Acknowledgements

GDL has received funding through the PRIN project "SACtoH2" (project code P2022AZETB by the Italian Ministry for Universities and Research (MUR), in the context of the National Recovery and Resilience Plan and co-financed by the European Commission - Next Generation EU (Mission 4, Component 1). Access to the CINECA supercomputing resources was granted via ISCRAB and EuroHPC Call Regular. We thank Alessandro Bonardi for useful discussions.

Supplementary materials

Supplementary material associated with this article can be found, in the online version, at doi:10.1016/j.electacta.2026.148733.

Data availability

The data reported in this article can be asked to the authors upon reasonable request.

References

[1] X.F. Yang, A. Wang, B. Qiao, J. Li, J. Liu, T. Zhang, Single-atom catalysts: a new frontier in heterogeneous catalysis, Acc. Chem. Res. 46 (2013) 1740–1748, https://doi.org/10.1021/ar300361m.

[2] A. Wang, J. Li, T. Zhang, Heterogeneous single-atom catalysis, Nat. Rev. Chem. 2 (2018) 65–81, https://doi.org/10.1038/s41570-018-0010-1.

[3] S.K. Kaiser, Z. Chen, D. Faust Akl, S. Mitchell, J. Pérez-Ramírez, Single-atom catalysts across the periodic table, Chem. Rev. 120 (2020) 11703–11809, https://doi.org/10.1021/acs.chemrev.0c00576.

[4] V.B. Saptal, V. Ruta, M.A. Bajada, G. Vilé, Single-atom catalysis in organic synthesis, Angew. Chem. Int. Ed. 62 (2023), https://doi.org/10.1002/anie.202219306.

[5] N. Cheng, L. Zhang, K. Doyle-Davis, X. Sun, Single-atom catalysts: from design to application, Electrochem. Energy Rev. 2 (2019) 539–573, https://doi.org/10.1007/s41918-019-00050-6.

[6] J. Liu, Catalysis by supported single metal atoms, ACS Catal. 7 (2017) 34–59, https://doi.org/10.1021/acscatal.6b01534.

[7] X. Cui, W. Li, P. Ryabchuk, K. Junge, M. Beller, Bridging homogeneous and heterogeneous catalysis by heterogeneous single-metal-site catalysts, Nat. Catal. 1 (2018) 385–397, https://doi.org/10.1038/s41929-018-0090-9.

[8] S.F. Yuk, G. Collinge, M.T. Nguyen, M.S. Lee, V.A. Glezakou, R. Rousseau, Single-atom catalysis: an analogy between heterogeneous and homogeneous catalysts, in: 2020: pp. 1–15. https://doi.org/10.1021/bk-2020-1360.ch001.

[9] Á. Morales-García, F. Calle-Vallejo, F. Illas, MXenes: new Horizons in catalysis, ACS Catal 10 (2020) 13487–13503, https://doi.org/10.1021/acscatal.0c03106.

[10] T. Li, T. Jing, D. Rao, S. Mourdikoudis, Y. Zuo, M. Wang, Two-dimensional materials for electrocatalysis and energy storage applications, Inorg. Chem. Front. 9 (2022) 6008–6046, https://doi.org/10.1039/D2QI01911F.

[11] D. Gupta, V. Chauhan, R. Kumar, A comprehensive review on synthesis and applications of molybdenum disulfide (MoS2) material: past and recent developments, Inorg. Chem. Commun. 121 (2020) 108200, https://doi.org/10.1016/j.inoche.2020.108200.

[12] Z. Wang, B. Mi, Environmental applications of 2D molybdenum disulfide (MoS_2) nanosheets, Environ. Sci. Technol. 51 (2017) 8229–8244, https://doi.org/10.1021/acs.est.7b01466.

[13] P.C.K. Vesborg, B. Seger, I. Chorkendorff, Recent development in hydrogen evolution reaction catalysts and their practical implementation, J. Phys. Chem. Lett. 6 (2015) 951–957, https://doi.org/10.1021/acs.jpclett.5b00306.

[14] H. Duan, C. Wang, G. Li, H. Tan, W. Hu, L. Cai, W. Liu, N. Li, Q. Ji, Y. Wang, Y. Lu, W. Yan, F. Hu, W. Zhang, Z. Sun, Z. Qi, L. Song, S. Wei, Single-atom-layer catalysis in a MoS_2 monolayer activated by long-range ferromagnetism for the hydrogen evolution reaction: beyond Single-atom catalysis, Angewandte Chemie. 133 (2021) 7327–7334, https://doi.org/10.1002/ange.202014968.

[15] Q. Li, X. Zhang, S. Dong, Y. Li, H. Zhao, H. Xie, Z. Wang, C. Zhou, Effects of doping and modulation on hydrogen evolution reaction of Pt@MoS2 single-atom catalysts: a first-principles study, Molecul. Catal. 549 (2023) 113485, https://doi.org/10.1016/j.mcat.2023.113485.

[16] J. Zhu, Y. Tu, L. Cai, H. Ma, Y. Chai, L. Zhang, W. Zhang, Defect-assisted anchoring of Pt single atoms on MoS_2 nanosheets produces high-performance catalyst for industrial hydrogen evolution reaction, Small 18 (2022), https://doi.org/10.1002/smll.202104824.

[17] Y. Ouyang, C. Ling, Q. Chen, Z. Wang, L. Shi, J. Wang, Activating inert basal planes of MoS_2 for hydrogen evolution reaction through the formation of different intrinsic defects, Chem. Mater. 28 (2016) 4390–4396, https://doi.org/10.1021/acs.chemmater.6b01395.

[18] C. Lang, W. Jiang, C. Yang, H. Zhong, P. Chen, Q. Wu, X. Yan, C. Dong, Y. Lin, L. Ouyang, Y. Jia, X. Yao, Facile and scalable mechanochemical synthesis of defective MoS_2 with Ru single atoms toward high-current-density hydrogen evolution, Small 19 (2023), https://doi.org/10.1002/smll.202300807.

[19] J. Deng, H. Li, J. Xiao, Y. Tu, D. Deng, H. Yang, H. Tian, J. Li, P. Ren, X. Bao, Triggering the electrocatalytic hydrogen evolution activity of the inert two-dimensional MoS_2 surface via single-atom metal doping, Energy Environ. Sci. 8 (2015) 1594–1601, https://doi.org/10.1039/C5EE00751H.

[20] Y. Ma, D. Leng, X. Zhang, J. Fu, C. Pi, Y. Zheng, B. Gao, X. Li, N. Li, P.K. Chu, Y. Luo, K. Huo, Enhanced activities in alkaline hydrogen and oxygen evolution reactions on MoS_2 electrocatalysts by In-plane sulfur defects coupled with transition metal doping, Small 18 (2022), https://doi.org/10.1002/smll.202203173.

[21] J. Zou, L. Li, N. Tan, K. Zhang, L. Wang, Z. Chen, Construction of S-scheme heterojunction with interfacial chemical bonds for enhanced photocatalytic CO2 reduction, Appl. Surf. Sci. 719 (2026) 165001, https://doi.org/10.1016/j.apsusc.2025.165001.

[22] N. Aguilar, M. Atilhan, S. Aparicio, Single atom transition metals on MoS2 monolayer and their use as catalysts for CO2 activation, Appl. Surf. Sci. 534 (2020) 147611, https://doi.org/10.1016/j.apsusc.2020.147611.

[23] Y. Ren, X. Sun, K. Qi, Z. Zhao, Single atom supported on MoS2 as efficient electrocatalysts for the CO2 reduction reaction: a DFT study, Appl. Surf. Sci. 602 (2022) 154211, https://doi.org/10.1016/j.apsusc.2022.154211.

[24] T. Yang, T.T. Song, J. Zhou, S. Wang, D. Chi, L. Shen, M. Yang, Y.P. Feng, High-throughput screening of transition metal single atom catalysts anchored on molybdenum disulfide for nitrogen fixation, Nano Energy 68 (2020) 104304, https://doi.org/10.1016/j.nanoen.2019.104304.

[25] L. Xu, M. Xie, H. Yang, P. Yu, B. Ma, T. Cheng, W.A. Goddard, In-silico screening the nitrogen reduction reaction on single-atom electrocatalysts anchored on MoS2, Top. Catal. 65 (2022) 234–241, https://doi.org/10.1007/s11244-021-01546-6.

[26] X. Zhai, L. Li, X. Liu, Y. Li, J. Yang, D. Yang, J. Zhang, H. Yan, G. Ge, A DFT screening of single transition atoms supported on MoS_2 as highly efficient electrocatalysts for the nitrogen reduction reaction, Nanoscale 12 (2020) 10035–10043, https://doi.org/10.1039/D0NR00030B.

[27] G. Tian, Z. Wang, C. Zhang, F. Wei, Nano bifunctional catalysts as miniaturized chemical processes for CO_x -to-aromatics conversion, Acc. Chem. Res. 59 (2026) 646–658, https://doi.org/10.1021/acs.accounts.5c00818.

[28] G. Di Liberto, L. Giordano, G. Pacchioni, Predicting the stability of single-atom catalysts in electrochemical reactions, ACS Catal 14 (2024) 45–55, https://doi.org/10.1021/acscatal.3c04801.

[29] L. Meng, F. Viñes, F. Illas, K.S. Exner, Stability of single-atom centers of MXenes under anodic polarization conditions, J. Phys. Chem. C 129 (2025) 9589–9601, https://doi.org/10.1021/acs.jpcc.5c01252.

[30] L. Meng, S. Razzaq, D. Singh, F. Viñes, F. Illas, K.S. Exner, Nitrogen embedding enhances stability and activity of single-atom motifs of MXenes under anodic polarization, NPJ 2D Mater. Appl. 9 (2025) 91, https://doi.org/10.1038/s41699-025-00610-z.

[31] Y. Jia, Y. Zhang, H. Xu, J. Li, M. Gao, X. Yang, Recent advances in doping strategies to improve electrocatalytic hydrogen evolution performance of molybdenum disulfide, ACS Catal 14 (2024) 4601–4637, https://doi.org/10.1021/acscatal.3c05053.

[32] X. Wang, Y. Zhang, J. Wu, Z. Zhang, Q. Liao, Z. Kang, Y. Zhang, Single-atom engineering to ignite 2D transition metal dichalcogenide based catalysis: fundamentals, progress, and beyond, Chem. Rev. 122 (2022) 1273–1348, https://doi.org/10.1021/acs.chemrev.1c00505.

[33] C. Du, H. Lin, B. Lin, Z. Ma, T. Hou, J. Tang, Y. Li, MoS_2 supported single platinum atoms and their superior catalytic activity for CO oxidation: a density functional theory study, J. Mater. Chem. A Mater. 3 (2015) 23113–23119, https://doi.org/10.1039/C5TA05084G.

[34] J. Zhang, X. Zhu, K. Zhu, J. Shen, Y. Xu, D. Chen, P. Wang, Adsorption of NO2 and NH3 on single-atom (Co, Pd, Pt)-decorated 2H-MoS2 monolayer: a DFT study, Results Phys 51 (2023) 106694, https://doi.org/10.1016/j.rinp.2023.106694.

[35] F. Ling, W. Xia, L. Li, X. Zhou, X. Luo, Q. Bu, J. Huang, X. Liu, W. Kang, M. Zhou, Single transition metal atom bound to the unconventional phase of the MoS_2 monolayer for catalytic oxygen reduction reaction: a first-principles study, ACS Appl. Mater. Interfaces 13 (2021) 17412–17419, https://doi.org/10.1021/acsami.0c21597.

[36] Y. Fan, J. Zhang, Y. Qiu, J. Zhu, Y. Zhang, G. Hu, A DFT study of transition metal (Fe, Co, Ni, Cu, Ag, Au, Rh, Pd, Pt and Ir)-embedded monolayer MoS2 for gas adsorption, Comput. Mater. Sci. 138 (2017) 255–266, https://doi.org/10.1016/j.commatsci.2017.06.029.

[37] J. Xu, J. Zhang, Z. Jiang, D. Wang, H. Li, Q. Liao, H. Shang, H. Xu, Transition metal single-atom doped MoS2 for gas adsorption: a combined density functional theory and machine learning study, Vacuum 240 (2025) 114566, https://doi.org/10.1016/j.vacuum.2025.114566.

[38] L.T. Phuong, S. Prabhakaran, D.H. Kim, Ni–P codoping engineered MoS_2 basal planes for electrocatalytic water splitting: insights from density functional theory, J. Mater. Chem. A Mater. 12 (2024) 28170–28176, https://doi.org/10.1039/D4TA04025B.

[39] Y. Wu, H. Wang, Z. Wu, X. Zhang, Y. Dong, Z. Hu, Y. Lv, X. Zhou, L. Zhao, B. Zhang, Q. Lu, Mechanism of NO electrocatalytic reduction over the MoS2-based single atom catalyst: a DFT investigation, Sep. Purif. Technol. 366 (2025) 132813, https://doi.org/10.1016/j.seppur.2025.132813.

[40] G. Kresse, J. Hafner, *Ab initio* molecular dynamics for liquid metals, Phys. Rev. B 47 (1993) 558–561, https://doi.org/10.1103/PhysRevB.47.558.

[41] G. Kresse, J. Hafner, *Ab initio* molecular-dynamics simulation of the liquid-metal–amorphous-semiconductor transition in germanium, Phys. Rev. B 49 (1994) 14251–14269, https://doi.org/10.1103/PhysRevB.49.14251.

[42] G. Kresse, J. Furthmüller, Efficiency of ab-initio total energy calculations for metals and semiconductors using a plane-wave basis set, Comput. Mater. Sci. 6 (1996) 15–50, https://doi.org/10.1016/0927-0256(96)00008-0.

[43] J.P. Perdew, K. Burke, M. Ernzerhof, Generalized gradient approximation made simple, Phys. Rev. Lett. 77 (1996) 3865–3868, https://doi.org/10.1103/PhysRevLett.77.3865.

[44] S. Grimme, J. Antony, S. Ehrlich, H. Krieg, A consistent and accurate *ab initio* parametrization of density functional dispersion correction (DFT-D) for the 94 elements H-Pu, J. Chem. Phys. 132 (2010), https://doi.org/10.1063/1.3382344.

[45] P.E. Blöchl, Projector augmented-wave method, Phys. Rev. B 50 (1994) 17953–17979, https://doi.org/10.1103/PhysRevB.50.17953.

[46] G. Kresse, D. Joubert, From ultrasoft pseudopotentials to the projector augmented-wave method, Phys. Rev. B 59 (1999) 1758–1775, https://doi.org/10.1103/PhysRevB.59.1758.

[47] S.A. Yamusa, A. Shaari, N.A.M. Alsaif, I.M. Alsalamah, I. Isah, N. Rekik, Elucidating the structural, electronic, elastic, and optical properties of bulk and monolayer MoS_2 transition-metal dichalcogenides: a DFT approach, ACS Omega 7 (2022) 45719–45731, https://doi.org/10.1021/acsomega.2c07030.

[48] V.A. Khalas, V.B. Parmar, A.M. Vora, A density Functional theory based study of transition metal dichalcogenide - MoS2, mater, Today Proc. 67 (2022) 165–169, https://doi.org/10.1016/j.matpr.2022.06.012.

[49] C. Adamo, V. Barone, Toward reliable density functional methods without adjustable parameters: the PBE0 model, J. Chem. Phys. 110 (1999) 6158–6170, https://doi.org/10.1063/1.478522.

[50] I. Barlocco, L.A. Cipriano, G. Di Liberto, G. Pacchioni, Modeling hydrogen and oxygen evolution reactions on single atom catalysts with density functional theory: role of the functional, Adv. Theory Simul. 6 (2023), https://doi.org/10.1002/adts.202200513.

[51] G. Di Liberto, L.A. Cipriano, G. Pacchioni, Universal principles for the rational design of single atom electrocatalysts? Handle with care, ACS Catal. 12 (2022) 5846–5856, https://doi.org/10.1021/acscatal.2c01011.

[52] D. Misra, G. Di Liberto, G. Pacchioni, CO2 electroreduction on single atom catalysts: is water just a solvent? J. Catal. 422 (2023) 1–11, https://doi.org/10.1016/j.jcat.2023.04.002.

[53] J.W. Furness, A.D. Kaplan, J. Ning, J.P. Perdew, J. Sun, Accurate and numerically efficient r^2 SCAN meta-generalized gradient approximation, J. Phys. Chem. Lett. 11 (2020) 8208–8215, https://doi.org/10.1021/acs.jpclett.0c02405.

[54] S. Faraji, Z. Wang, P. Lopez-Rivera, M. Liu, Advancements in computational approaches for rapid metal site discovery in carbon-based materials for electrocatalysis, Energy Adv. 2 (2023) 1781–1799, https://doi.org/10.1039/D3YA00321C.

[55] M. Spotti, G. Di Liberto, G. Pacchioni, CO2 Activation on single-atom catalysts: importance of the supporting matrix, Top. Catal. 68 (2025) 1837–1847, https://doi.org/10.1007/s11244-025-02064-5.
[56] Y.Q. Su, L. Zhang, Y. Wang, J.X. Liu, V. Muravev, K. Alexopoulos, I.A.W. Filot, D. G. Vlachos, E.J.M. Hensen, Stability of heterogeneous single-atom catalysts: a scaling law mapping thermodynamics to kinetics, NPJ Comput. Mater. 6 (2020) 144, https://doi.org/10.1038/s41524-020-00411-6.
[57] J.K. Nørskov, T. Bligaard, A. Logadottir, J.R. Kitchin, J.G. Chen, S. Pandelov, U. Stimming, Trends in the exchange current for hydrogen evolution, J. Electrochem. Soc. 152 (2005) J23, https://doi.org/10.1149/1.1856988.
[58] J.K. Nørskov, J. Rossmeisl, A. Logadottir, L. Lindqvist, J.R. Kitchin, T. Bligaard, H. Jónsson, Origin of the overpotential for oxygen reduction at a fuel-cell cathode, J. Phys. Chem. B 108 (2004) 17886–17892, https://doi.org/10.1021/jp047349j.
[59] E. Di Simone, G. Vilé, G. Di Liberto, G. Pacchioni, Decoding the role of adsorbates entropy in the reactivity of single-atom catalysts, ACS Catal 15 (2025) 447–456, https://doi.org/10.1021/acscatal.4c04472.
[60] C. Saetta, I. Barlocco, G. Di Liberto, G. Pacchioni, Key ingredients for the screening of single atom catalysts for the hydrogen evolution reaction: the case of titanium nitride, Small 20 (2024), https://doi.org/10.1002/smll.202401058.
[61] S. Picello, E. Inico, C. Saetta, G. Di Liberto, G. Pacchioni, Single-atom catalysts on goldene, ACS Catal 15 (2025) 11232–11242, https://doi.org/10.1021/acscatal.5c01820.
[62] K. Mathew, R. Sundararaman, K. Letchworth-Weaver, T.A. Arias, R.G. Hennig, Implicit solvation model for density-functional study of nanocrystal surfaces and reaction pathways, J. Chem. Phys. 140 (2014), https://doi.org/10.1063/1.4865107.
[63] K. Mathew, V.S.C. Kolluru, S. Mula, S.N. Steinmann, R.G. Hennig, Implicit self-consistent electrolyte model in plane-wave density-functional theory, J. Chem. Phys. 151 (2019), https://doi.org/10.1063/1.5132354.
[64] M.C.O. Monteiro, F. Dattila, N. López, M.T.M. Koper, The role of cation acidity on the competition between hydrogen evolution and CO $_2$ reduction on gold electrodes, J. Am. Chem. Soc. 144 (2022) 1589–1602, https://doi.org/10.1021/jacs.1c10171.
[65] M.C.O. Monteiro, F. Dattila, B. Hagedoorn, R. García-Muelas, N. López, M.T. M. Koper, Absence of CO2 electroreduction on copper, gold and silver electrodes without metal cations in solution, Nat. Catal. 4 (2021) 654–662, https://doi.org/10.1038/s41929-021-00655-5.
[66] J.T. Bender, A.S. Petersen, F.C. Østergaard, M.A. Wood, S.M.J. Heffernan, D. J. Milliron, J. Rossmeisl, J. Resasco, Understanding cation effects on the hydrogen evolution reaction, ACS Energy Lett 8 (2023) 657–665, https://doi.org/10.1021/acsenergylett.2c02500.
[67] G. Di Liberto, L. Giordano, Role of solvation model on the stability of oxygenates on Pt(111): a comparison between microsolvation, extended bilayer, and extended metal/water interface, Electrochem. Sci. Adv. 4 (2024), https://doi.org/10.1002/elsa.202100204.
[68] L.M. Azofra, C. Sun, L. Cavallo, D.R. MacFarlane, Feasibility of N $_2$ binding and reduction to ammonia on Fe-deposited MoS $_2$ 2D sheets: a DFT study, Chem. – A European J. 23 (2017) 8275–8279, https://doi.org/10.1002/chem.201701113.
[69] R. Sundararaman, W.A. Goddard, T.A. Arias, Grand canonical electronic density-functional theory: algorithms and applications to electrochemistry, J. Chem. Phys. 146 (2017), https://doi.org/10.1063/1.4978411.
[70] Y. Huang, R.J. Nielsen, W.A. Goddard, Reaction mechanism for the hydrogen evolution Reaction on the basal plane sulfur vacancy site of MoS $_2$ using grand canonical potential kinetics, J. Am. Chem. Soc. 140 (2018) 16773–16782, https://doi.org/10.1021/jacs.8b10016.
[71] S. Osella, W.A. Goddard, CO $_2$ reduction to methane and ethylene on a single-atom catalyst: a grand canonical Quantum Mechanics study, J. Am. Chem. Soc. 145 (2023) 21319–21329, https://doi.org/10.1021/jacs.3c05650.
[72] P. Delahay, M. Pourbaix, P. Van Rysselberghe, Potential-pH diagram of lead and its applications to the study of lead corrosion and to the lead storage battery, J. Electrochem. Soc. 98 (1951) 57.
[73] M. Pourbaix, Applications of electrochemistry in corrosion science and in practice, Corros. Sci. 14 (1974) 25–82.
[74] P. Janthon, S.(Andy) Luo, S.M. Kozlov, F. Viñes, J. Limtrakul, D.G. Truhlar, F. Illas, Bulk properties of transition metals: a challenge for the design of universal density functionals, J. Chem. Theory Comput. 10 (2014) 3832–3839, https://doi.org/10.1021/ct500532v.
[75] B. Singh, M.B. Gawande, A.D. Kute, R.S. Varma, P. Fornasiero, P. McNeice, R. V. Jagadeesh, M. Beller, R. Zbořil, Single-atom (Iron-Based) catalysts: synthesis and applications, Chem. Rev. 121 (2021) 13620–13697, https://doi.org/10.1021/acs.chemrev.1c00158.
[76] A. Walsh, A.A. Sokol, J. Buckeridge, D.O. Scanlon, C.R.A. Catlow, Electron counting in solids: oxidation states, partial charges, and ionicity, J. Phys. Chem. Lett. 8 (2017) 2074–2075, https://doi.org/10.1021/acs.jpclett.7b00809.
[77] C. Chowdhury, M. Lovato, G. Di Liberto, F. Viñes, F. Illas, G. Pacchioni, L. Giordano, Predicting the HER activity of SACs on MXenes with simple features and interpretable machine learning models, J. Mater. Chem. A Mater. 14 (2026) 5349–5365, https://doi.org/10.1039/D5TA07143G.
[78] T.F. Jaramillo, K.P. Jørgensen, J. Bonde, J.H. Nielsen, S. Horch, I. Chorkendorff, Identification of active edge sites for electrochemical H $_2$ evolution from MoS $_2$ nanocatalysts, Science (1979) 317 (2007) 100–102, https://doi.org/10.1126/science.1141483.
[79] Z. Wang, Q. Li, H. Xu, C. Dahl-Petersen, Q. Yang, D. Cheng, D. Cao, F. Besenbacher, J.V. Lauritsen, S. Helveg, M. Dong, Controllable etching of MoS2 basal planes for enhanced hydrogen evolution through the formation of active edge sites, Nano Energy 49 (2018) 634–643, https://doi.org/10.1016/j.nanoen.2018.04.067.
[80] G. Di Liberto, G. Pacchioni, Modeling single-atom catalysis, Adv. Mater. 35 (2023) 2307150, https://doi.org/10.1002/adma.202307150.
[81] G. Di Liberto, S. Tosoni, L.A. Cipriano, G. Pacchioni, A few questions about single-atom catalysts: when modeling helps, Acc. Mater. Res. 3 (2022) 986–995, https://doi.org/10.1021/accountsmr.2c00118.
[82] X. Han, Q. Liu, A. Qian, L. Ye, X. Pu, J. Liu, X. Jia, R. Wang, F. Ju, H. Sun, J. Zhao, H. Ling, Transition-metal single atom anchored on MoS $_2$ for enhancing photocatalytic hydrogen production of g-C $_3$ N $_4$ photocatalysts, ACS Appl. Mater. Interfaces 15 (2023) 26670–26681, https://doi.org/10.1021/acsami.3c02895.
[83] Z. Li, D. Liao, G. Tian, X. Fan, X. Chai, W. Chang, Y. Gao, B. Yuan, Z. Li, F. Wei, C. Zhang, Determination of Mn valence states in nanocatalysts during sustainable Syngas conversion, J. Am. Chem. Soc. 147 (2025) 32548–32559, https://doi.org/10.1021/jacs.5c06550.